

Electronic Supplementary Information for:

**Highly efficient reduction of carbon dioxide with a borane catalyzed
by bis(phosphinite) pincer ligated palladium thiolate complexes**

Qiang-Qiang Ma,^a Ting Liu,^a Shujun Li,^a Jie Zhang,^{*a} Xuenian Chen^{*a} and Hairong Guan^{*b}

^aSchool of Chemistry and Chemical Engineering, Henan Key Laboratory of Boron Chemistry and Advanced Energy Materials, Henan Normal University, Xinxiang, Henan 453007, China.

^bDepartment of Chemistry, University of Cincinnati, P. O. Box 210172, Cincinnati, OH 45221-0172,
USA

E-mails: jie.zhang@htu.edu.cn (J.Z.); xnchen@htu.edu.cn (X.C.); hairong.guan@uc.edu (H.G.)

General information for synthesis and characterization.....	1
Syntheses of [2,6-(R ₂ PO) ₂ C ₆ H ₃]PdSY (1-4).....	1-3
X-ray structure determination of complexes 1 , 2 and 3	3
Table S1 Summary of crystal data and structure refinement for complexes 1 , 2 and 3	4
Fig. S1: ORTEP drawing of complex 2	4
Table S2-S4: Bond lengths and angles for complexes 1 , 2 and 3	5-8
Catalytic hydroboration of CO ₂ with complexes 1 , 2 and 3	9
Figs S2-S7: NMR spectra for catalytic hydroboration of CO ₂	10-12

General information for synthesis and characterization

Unless otherwise indicated, all the syntheses were carried out under a nitrogen atmosphere using standard Schlenk and glove box techniques. Solvents used for the reactions were degassed and dried using standard procedures. Benzene-*d*₆ was distilled from Na and benzophenone under a nitrogen atmosphere. Catecholborane was purchased from Sigma-Aldrich and purified by vacuum distillation. ¹H, ¹¹B and ³¹P NMR spectra were recorded on a Bruker Advance 400 MHz spectrometer. ¹³C NMR spectra were recorded on a Bruker Advance 400 MHz or a Bruker AVANCE III 600 MHz spectrometer. Mass spectra were performed on a Bruker micrOTOF II instrument. Palladium chloride complexes [2,6-(R₂PO)₂C₆H₃]PdCl (R = ^tBu, ⁱPr, Ph) were synthesized according to published procedures.¹⁻³

Synthesis of [2,6-(ⁱPr₂PO)₂C₆H₃]PdSPh (1)

To a suspension of NaH (240 mg, 10.0 mmol) in 20 mL of THF was added thiophenol dropwise (1.0 mL, 10.0 mmol) at 0 °C under a nitrogen atmosphere. The resulting mixture was warmed to room temperature and stirred for 1 h. A solution of [2,6-(ⁱPr₂PO)₂C₆H₃]PdCl (966.5 mg, 2 mmol) in THF (10 mL) was then added. The mixture was refluxed under a nitrogen atmosphere for 36 h. After cooling to room temperature, the mixture was filtered through a pad of Celite and the volatiles were removed under vacuum. The residue was extracted with hexane for three times (20 mL × 3) and the combined hexane solution was concentrated followed by recrystallization to produce complex **1** as an orange crystalline solid (947 mg, 85% yield). ¹H NMR (400 MHz, CDCl₃, δ): 7.46 (d, 2H, ArH, *J* = 7.2 Hz), 6.95-7.02 (m, 3H, ArH), 6.90 (t, 1H, ArH, *J* = 7.4 Hz), 6.56 (d, 2H, ArH, *J* = 7.9 Hz), 2.09-2.20 (m, 4H, CH(CH₃)₂), 1.20–1.28 (m, 24H, CH(CH₃)₂). ¹³C{¹H} NMR (101 MHz, CDCl₃, δ): 165.88 (t, ArC, *J* = 6.2 Hz), 148.20 (t, ArC, *J* = 4.4 Hz), 134.73 (t, ArC, *J* = 4.3 Hz), 134.06 (s, ArC), 128.12 (s, ArC), 127.36 (s, ArC), 122.73 (s, ArC), 105.58 (t, ArC, *J* = 7.0 Hz), 29.13 (t, CH(CH₃)₂, *J* = 12.0 Hz), 17.32 (t, CH(CH₃)₂, *J* = 3.3 Hz), 16.74 (s, CH(CH₃)₂). ¹³C{¹H} NMR (151 MHz, C₆D₆, δ): 166.41 (t, ArC, *J* = 6.4 Hz), 150.66 (t, ArC, *J* = 4.5 Hz), 135.63 (t, ArC, *J* = 3.6 Hz), 134.52 (s, ArC), 128.35 (s, ArC), 127.53 (s, ArC), 122.58 (s, ArC), 106.03 (t, *J* = 6.9 Hz, ArC), 29.30 (t, CH(CH₃)₂, *J* = 11.1 Hz), 17.25 (t, CH(CH₃)₂, *J* = 3.3 Hz), 16.63 (s, CH(CH₃)₂). ³¹P{¹H} NMR (162 MHz, C₆D₆, δ): 189.69 (s). HRMS (ESI): m/z Calculated for C₂₄H₃₆O₂P₂PdS + Na⁺ [M + Na]⁺ 579.0854, found 579.0847.

Synthesis of [2,6-(^tBu₂PO)₂C₆H₃]PdSPh (2)

Complex **2** was prepared from [2,6-(^tBu₂PO)₂C₆H₃]PdCl, thiophenol and NaH in 80% yield as a bright yellow crystalline solid by procedures similar to those used for complex **1**. ¹H NMR (400 MHz, CDCl₃, δ): 7.47 (d, 2H, ArH, *J* = 7.1 Hz), 6.95–7.00 (m, 3H, ArH), 6.87 (t, 1H, ArH, *J* = 7.1 Hz), 6.56 (d, 2H, ArH, *J* = 7.6 Hz), 1.31–1.33 (m, 36H, C(CH₃)₃). ¹³C{¹H} NMR (151 MHz, C₆D₆, δ): 167.12 (t, ArC, *J* = 5.5 Hz), 149.85 (t, ArC, *J* = 1.8 Hz), 135.30 (t, ArC, *J* = 2.5 Hz), 134.57 (s, ArC), 128.58 (s, ArC), 128.35 (s, ArC), 122.13 (s, ArC), 105.74 (t, ArC, *J* = 7.1 Hz), 39.98 (t, C(CH₃)₃, *J* = 7.7 Hz), 27.81 (t, C(CH₃)₃, *J* = 3.6 Hz). ³¹P{¹H} NMR (162 MHz, C₆D₆, δ): 192.36 (s). HRMS (ESI): m/z Calculated for C₂₈H₄₄O₂P₂PdS + Na⁺ [M + Na]⁺ 635.1482, found 635.1475.

Synthesis of [2,6-(Ph₂PO)₂C₆H₃]PdSPh (3)

Complex **3** was prepared from [2,6-(Ph₂PO)₂C₆H₃]PdCl, thiophenol and NaH as a yellow crystalline solid in 80% yield by procedures similar to those used for complex **1**. ¹H NMR (400 MHz, CDCl₃, δ): 7.76–7.80 (m, 8H, ArH), 7.33–7.48 (m, 12H, ArH), 7.06 – 7.18 (m, 3H, ArH), 6.77 (d, 2H, ArH, *J* = 8.0 Hz), 6.61 (t, 1H, ArH, *J* = 7.3 Hz), 6.52 (t, 2H, ArH, *J* = 7.6 Hz). ¹³C{¹H} NMR (151 MHz, C₆D₆, δ): 164.84 (t, ArC, *J* = 7.6 Hz), 148.12 (t, ArC, *J* = 3.7 Hz), 138.08 (t, ArC, *J* = 5.0 Hz), 134.15 (t, ArC, *J* = 25.8 Hz), 134.10 (s, ArC), 132.32 (t, ArC, *J* = 8.2 Hz), 131.75 (s, ArC), 128.94 (t, ArC, *J* = 5.1 Hz), 128.39 (s, ArC), 127.62 (s, ArC), 122.29 (s, ArC), 107.38 (t, ArC, *J* = 7.8 Hz). ³¹P{¹H} NMR (162 MHz, CDCl₃, δ): 147.78 (s). HRMS (ESI): m/z Calculated for C₃₆H₂₈O₂P₂PdS + Na⁺ [M + Na]⁺ 715.0225, found 715.0225.

Synthesis of [2,6-(ⁱPr₂PO)₂C₆H₃]PdSCH₂Ph (4)

Complex **4** was prepared from [2,6-(ⁱPr₂PO)₂C₆H₃]PdCl, benzenemethanethiol and NaH as a pale yellow crystalline solid in 78% yield by procedures similar to those used for complex **1**. ¹H NMR (400 MHz, CDCl₃, δ): 7.41 (d, 2H, ArH, *J* = 7.4 Hz), 7.22 – 7.26 (m, 2H, ArH), 7.12 (t, 1H, ArH, *J* = 5.6 Hz), 6.95 (t, 1H, ArH, *J* = 8.0 Hz), 6.56 (d, 2H, ArH, *J* = 7.9 Hz), 3.89 (s, 2H, CH₂), 2.34–2.41(m, 4H, CH(CH₃)₂), 1.24 – 1.38 (m, 24H, CH(CH₃)₂). ¹³C{¹H} NMR (151 MHz, C₆D₆, δ): 166.03 (t, ArC, *J* = 6.6 Hz), 147.07 (s, ArC), 136.67 (s, ArC), 131.65 (s, ArC), 129.08 (s, ArC), 128.35 (s, ArC), 125.98 (s, ArC), 105.92 (t, ArC, *J* = 7.1 Hz), 38.88 (t, SCH₂, *J* = 7.2 Hz), 29.51 (t, CH(CH₃)₂, *J* = 11.9 Hz), 17.31 (t, CH(CH₃)₂, *J* = 3.5 Hz), 16.66 (s, CH(CH₃)₂). ³¹P{¹H} NMR (162

MHz, CDCl₃, δ): 191.39 (s). HRMS (ESI): m/z Calculated for C₂₅H₃₈O₂P₂PdS + Na⁺ [M + Na]⁺ 593.1004, found 593.1004.

X-ray structure determination of complexes **1**, **2** and **3**

Single crystals of complexes **1**, **2** and **3** were obtained from crystallization in *n*-hexane. Intensity data were collected at 296 K on a Bruker SMART6000 CCD diffractometer using graphite-monochromated MoKα radiation, λ = 0.71073 Å. The frames were integrated with the Bruker APEX2 software package using a narrow-frame algorithm. The data were corrected for decay, Lorentz, and polarization effects as well as absorption and beam corrections based on the multi-scan technique. The structures were solved by a combination of direct methods in SHELXTL and the difference Fourier technique and refined by full-matrix least-squares procedures. Nonhydrogen atoms were refined with anisotropic displacement parameters. The H-atoms were either located or calculated and subsequently treated with a riding model. No solvent of crystallization is present in the lattice for any of the structures. Crystal data collection and refinement parameters are summarized in Table S1. The structure of **2** is shown in Figs S1; bond lengths and angles are provided in Tables S2-S4 respectively.

Table S1 Summary of crystal data and structure refinement for complexes **1**, **2** and **3**

	1	2	3
Empirical formula	C ₂₄ H ₃₆ O ₂ P ₂ PdS	C ₂₈ H ₄₄ O ₂ P ₂ PdS	C ₃₆ H ₂₈ O ₂ P ₂ PdS
Formula weight	556.93	613.03	692.98
Temp, K	296(2)	296(2)	296(2)
Crystal system	Triclinic	Triclinic	Triclinic
Space group	P -1	P -1	P -1
<i>a</i> , Å	8.7065(15)	8.6167(9)	9.0944(7)
<i>b</i> , Å	11.0937(19)	11.5992(12)	11.4218(9)
<i>c</i> , Å	15.130(3)	16.4263(17)	15.9032(12)
α (°)	73.3056(17)	77.1791(12)	95.9441(8)
β (°)	80.9582(19)	79.8629(14)	103.4741(8)
γ (°)	74.8990(18)	73.9166(13)	102.0487(8)
Volume, Å ³	1346.1(4)	1526.6(3)	1550.8(2)
Z	2	2	2
<i>d</i> _{calc} , g cm ⁻³	1.374	1.334	1.484
λ , Å	0.71073	0.71073	0.71073
μ , mm ⁻¹	0.903	0.803	0.801
No. of data collected	4807	7086	7119
No. of unique data	4369	4867	5718
<i>R</i> _{int}	0.0172	0.0350	0.0175
Goodness-of-fit on <i>F</i> ²	1.015	1.088	1.055
<i>R</i> ₁ , w <i>R</i> ₂ (<i>I</i> > 2σ(<i>I</i>))	0.0235, 0.0657	0.0481, 0.0950	0.0325, 0.0805
<i>R</i> ₁ , w <i>R</i> ₂ (all data)	0.0286, 0.0757	0.0776, 0.1175	0.0401, 0.0879

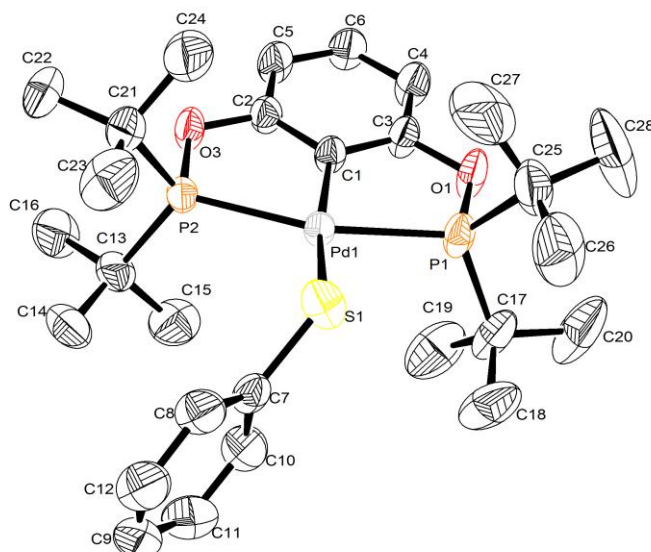


Figure S1 ORTEP drawing of [2,6-(^tBu₂PO)₂C₆H₃]PdSPh (**2**) at the 50 % probability level. Hydrogen atoms are omitted for clarity.

Table S2 Bond lengths (Å) and angles (°) for complex **1**

C1-C23	1.368(6)	C12-C18	1.518(4)
C1-C15	1.382(5)	C12-C22	1.529(5)
C2-C4	1.518(4)	C12-P1	1.823(3)
C2-C3	1.529(5)	C13-C20	1.526(5)
C2-P2	1.830(3)	C13-C24	1.528(5)
C5-C6	1.391(3)	C13-P1	1.827(3)
C5-C7	1.391(3)	C14-C25	1.512(6)
C5-Pd1	2.015(2)	C14-C21	1.536(4)
C6-C10	1.380(4)	C14-P2	1.827(3)
C6-O1	1.397(3)	C16-C19	1.386(5)
C7-C11	1.385(4)	C19-C23	1.361(5)
C7-O2	1.393(3)	O2-P2	1.6558(19)
C8-C15	1.385(4)	O1-P1	1.6570(18)
C8-C16	1.385(4)	P1-Pd1	2.2775(7)
C8-S1	1.772(3)	P2-Pd1	2.2871(6)
C10-C17	1.387(4)	Pd1-S1	2.3674(7)
C11-C17	1.381(4)		
C23-C1-C15	121.3(4)	C1-C15-C8	120.4(3)
C4-C2-C3	111.0(3)	C8-C16-C19	120.9(3)
C4-C2-P2	114.9(2)	C11-C17-C10	121.6(3)
C3-C2-P2	108.7(2)	C23-C19-C16	120.8(3)
C6-C5-C7	116.4(2)	C19-C23-C1	118.8(3)
C6-C5-Pd1	121.19(18)	C7-O2-P2	114.47(15)
C7-C5-Pd1	122.39(18)	C6-O1-P1	114.79(15)
C10-C6-C5	122.8(2)	O1-P1-C12	102.89(11)
C10-C6-O1	118.5(2)	O1-P1-C13	101.11(13)
C5-C6-O1	118.7(2)	C12-P1-C13	107.21(13)
C11-C7-C5	122.9(2)	O1-P1-Pd1	105.04(6)
C11-C7-O2	119.1(2)	C12-P1-Pd1	116.15(9)
C5-C7-O2	117.9(2)	C13-P1-Pd1	121.60(10)
C15-C8-C16	117.7(3)	O2-P2-C14	101.90(13)
C15-C8-S1	119.7(2)	O2-P2-C2	100.52(12)
C16-C8-S1	122.5(2)	C14-P2-C2	107.91(14)
C6-C10-C17	118.3(3)	O2-P2-Pd1	105.31(7)
C17-C11-C7	118.0(2)	C14-P2-Pd1	113.56(10)
C18-C12-C22	111.5(3)	C2-P2-Pd1	124.33(10)
C18-C12-P1	113.5(2)	C5-Pd1-P1	80.27(7)
C22-C12-P1	109.6(2)	C5-Pd1-P2	79.16(7)
C20-C13-C24	112.5(4)	P1-Pd1-P2	158.25(3)
C20-C13-P1	110.7(2)	C5-Pd1-S1	174.54(7)
C24-C13-P1	109.2(2)	P1-Pd1-S1	95.26(3)
C25-C14-C21	111.9(3)	P2-Pd1-S1	104.85(3)

C25-C14-P2	110.4(3)	C8-S1-Pd1	109.98(8)
C21-C14-P2	109.6(2)		

Table S3 Bond lengths (\AA) and angles ($^{\circ}$) for complex **2**

Pd1-C1	2.000(4)	C7-C8	1.382(6)
Pd1-P1	2.2833(12)	C13-C14	1.529(7)
Pd1-P2	2.3193(11)	C13-C16	1.535(7)
Pd1-S1	2.3745(12)	C13-C15	1.545(7)
P2-O3	1.654(3)	C21-C23	1.516(7)
P2-C21	1.862(5)	C21-C22	1.528(7)
P2-C13	1.869(5)	C21-C24	1.539(7)
P1-O1	1.653(3)	C5-C6	1.372(6)
P1-C25	1.841(6)	C17-C18	1.525(7)
P1-C17	1.880(6)	C17-C19	1.525(9)
S1-C7	1.752(5)	C17-C20	1.532(7)
O3-C2	1.390(5)	C8-C12	1.381(7)
O1-C3	1.393(5)	C9-C12	1.360(8)
C1-C2	1.386(5)	C9-C11	1.385(8)
C1-C3	1.393(6)	C10-C11	1.373(7)
C2-C5	1.389(6)	C25-C26	1.527(8)
C3-C4	1.372(6)	C25-C27	1.532(10)
C4-C6	1.386(6)	C25-C28	1.542(8)
C7-C10	1.374(7)		
C1-Pd1-P1	80.15(12)	C8-C7-S1	118.5(4)
C1-Pd1-P2	79.70(12)	C14-C13-C16	109.4(4)
P1-Pd1-P2	159.79(4)	C14-C13-C15	110.0(4)
C1-Pd1-S1	168.53(13)	C16-C13-C15	108.5(5)
P1-Pd1-S1	94.31(4)	C14-C13-P2	110.9(4)
P2-Pd1-S1	105.80(4)	C16-C13-P2	113.1(4)
O3-P2-C21	100.7(2)	C15-C13-P2	104.9(3)
O3-P2-C13	99.6(2)	C23-C21-C22	110.8(4)
C21-P2-C13	113.4(2)	C23-C21-C24	108.2(5)
O3-P2-Pd1	103.65(11)	C22-C21-C24	109.3(4)
C21-P2-Pd1	116.22(17)	C23-C21-P2	110.9(4)
C13-P2-Pd1	119.05(16)	C22-C21-P2	113.3(4)
O1-P1-C25	100.7(2)	C24-C21-P2	104.1(3)
O1-P1-C17	101.3(2)	C6-C5-C2	119.3(4)
C25-P1-C17	114.3(3)	C5-C6-C4	120.6(4)
O1-P1-Pd1	104.49(11)	C18-C17-C19	109.2(6)
C25-P1-Pd1	118.4(2)	C18-C17-C20	109.7(4)
C17-P1-Pd1	114.42(19)	C19-C17-C20	109.0(5)
C7-S1-Pd1	113.45(16)	C18-C17-P1	110.4(4)
C2-O3-P2	115.8(2)	C19-C17-P1	105.0(3)

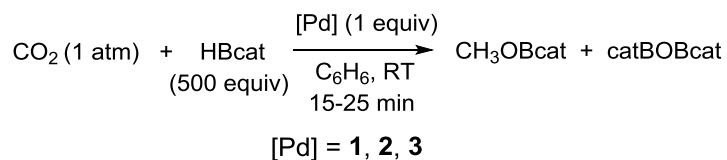
C3-O1-P1	115.6(3)	C20-C17-P1	113.4(5)
C2-C1-C3	115.4(4)	C12-C8-C7	120.3(5)
C2-C1-Pd1	122.3(3)	C12-C9-C11	118.8(5)
C3-C1-Pd1	122.0(3)	C11-C10-C7	121.5(5)
C1-C2-O3	118.2(4)	C10-C11-C9	120.0(6)
C1-C2-C5	122.5(4)	C9-C12-C8	121.2(5)
O3-C2-C5	119.2(4)	C26-C25-C27	106.2(6)
C4-C3-O1	118.3(4)	C26-C25-C28	110.4(5)
C4-C3-C1	124.1(4)	C27-C25-C28	110.2(6)
O1-C3-C1	117.6(4)	C26-C25-P1	112.2(4)
C3-C4-C6	118.1(4)	C27 C25 P1	104.1(4)
C10-C7-C8	118.2(5)	C28 C25 P1	113.3(5)
C10-C7-S1	123.3(4)		

Table S4 Bond lengths (\AA) and angles ($^{\circ}$) for complex **3**

C1-C6	1.380(4)	C20-C21	1.389(5)
C1-C2	1.393(4)	C21-C22	1.388(4)
C1-Pd1	2.014(3)	C22-C23	1.389(4)
C2-C3	1.386(4)	C22-P1	1.804(3)
C2-O2	1.396(3)	C23-C24	1.381(5)
C3-C5	1.383(4)	C25-C26	1.367(6)
C4-C6	1.384(4)	C25-C29	1.387(5)
C4-C5	1.390(4)	C26-C27	1.354(6)
C6-O1	1.393(3)	C27-C28	1.384(5)
C7-C12	1.375(5)	C28-C30	1.383(4)
C7-C8	1.382(5)	C29-C30	1.392(4)
C7-P2	1.802(3)	C30-P1	1.807(3)
C8-C9	1.373(7)	C60-C65	1.338(6)
C9-C10	1.370(8)	C60-C6	1.1.378(6)
C10-C11	1.365(8)	C60-S1	1.778(4)
C11-C12	1.384(5)	C61-C62	1.387(6)
C13-C18	1.381(4)	C62-C63	1.350(9)
C13-C14	1.383(4)	C63-C64	1.327(13)
C13-P2	1.806(3)	C64-C65	1.395(9)
C14-C15	1.381(5)	O1-P1	1.6559(19)
C15-C16	1.355(6)	O2-P2	1.648(2)
C16-C17	1.360(7)	P1-Pd1	2.2867(7)
C17-C18	1.411(6)	P2-Pd1	2.2677(7)
C19-C20	1.361(5)	Pd1-S1	2.3635(8)
C19-C24	1.372(5)		
C6-C1-C2	116.8(2)	C27-C26-C25	120.2(4)
C6-C1-Pd1	122.03(19)	C26-C27-C28	120.5(4)
C2-C1-Pd1	121.16(19)	C30-C28-C27	120.3(3)

C3-C2-C1	122.6(3)	C25-C29-C30	119.8(4)
C3-C2-O2	118.9(2)	C28-C30-C29	118.7(3)
C1-C2-O2	118.5(2)	C28-C30-P1	122.8(2)
C5-C3-C2	118.2(3)	C29-C30-P1	118.4(2)
C6-C4-C5	118.3(3)	C65-C60-C61	117.8(4)
C3-C5-C4	121.2(3)	C65-C60-S1	118.8(4)
C1-C6-C4	122.8(2)	C61-C60-S1	123.3(3)
C1-C6-O1	118.4(2)	C60-C61-C62	121.8(5)
C4-C6-O1	118.7(2)	C63-C62-C61	118.5(6)
C12-C7-C8	119.2(3)	C64-C63-C62	120.0(6)
C12-C7-P2	118.8(3)	C63-C64-C65	121.6(7)
C8-C7-P2	122.0(3)	C60-C65-C64	119.9(7)
C9-C8-C7	119.6(5)	C6-O1-P1	114.28(16)
C10-C9-C8	121.0(5)	C2-O2-P2	113.69(16)
C11-C10-C9	119.8(4)	O1-P1-C22	102.74(12)
C10-C11-C12	119.6(5)	O1-P1-C30	99.79(11)
C7-C12-C11	120.7(4)	C22-P1-C30	106.92(12)
C18-C13-C14	119.6(3)	O1-P1-Pd1	104.82(7)
C18-C13-P2	119.0(3)	C22-P1-Pd1	115.38(9)
C14-C13-P2	121.2(2)	C30-P1-Pd1	123.84(10)
C15-C14-C13	120.8(3)	O2-P2-C7	101.47(13)
C16-C15-C14	119.6(4)	O2-P2-C13	101.91(12)
C15-C16-C17	121.2(4)	C7-P2-C13	106.08(13)
C16-C17-C18	120.1(4)	O2-P2-Pd1	105.56(7)
C13-C18-C17	118.7(4)	C7-P2-Pd1	124.28(10)
C20-C19-C24	120.2(3)	C13-P2-Pd1	114.45(10)
C19-C20-C21	120.7(3)	C1-Pd1-P2	79.62(8)
C22-C21-C20	119.8(3)	C1-Pd1-P1	79.37(8)
C21-C22-C23	118.8(3)	P2-Pd1-P1	158.94(3)
C21-C22-P1	119.1(2)	C1-Pd1-S1	175.08(8)
C23-C22-P1	121.9(2)	P2-Pd1-S1	96.30(3)
C24-C23-C22	120.4(3)	P1-Pd1-S1	104.75(3)
C19-C24-C23	120.1(4)	C60-S1-Pd1	109.66(11)
C26-C25-C29	120.3(4)		

Catalytic hydroboration of CO₂ with complexes **1**, **2** and **3**



Catalytic hydroboration of carbon dioxide was carried out under 1 atm of CO₂ at room temperature in benzene with a catalyst to substrate ratio of 1:500. Typically, 0.011 mmol of the palladium thiolate complex, 5.50 mmol of catecholborane (HBcat), 0.022 mmol of hexamethylbenzene (as an internal standard) and 4 mL of benzene were mixed in a flame-dried 50 mL Schlenk flask under a nitrogen atmosphere, and then CO₂ was bubbled through the solution. The resulting solution was stirred under 1 atm of CO₂ at room temperature until the temperature of the reaction mixture increased to 40-50 °C and a large amount of white precipitate developed. The mixture was stirred for another 2 min and cooled to room temperature. The resulting white precipitate was allowed to settle, and 0.6 mL of the clear liquid was transferred under nitrogen into an NMR tube and ¹¹B NMR spectra were taken. ¹H NMR spectra were taken by mixing 0.3 mL of the clear solution with 0.3 mL of benzene-*d*₆ in an NMR tube. Turnover number (TON) was calculated based on B–H bond by comparing the ¹H NMR integration of the CH₃OBcat methyl resonance (3.38 ppm) with that of the internal standard (2.11 ppm). ¹H NMR and ¹¹B NMR spectra are provided in Figs S2 to S7.

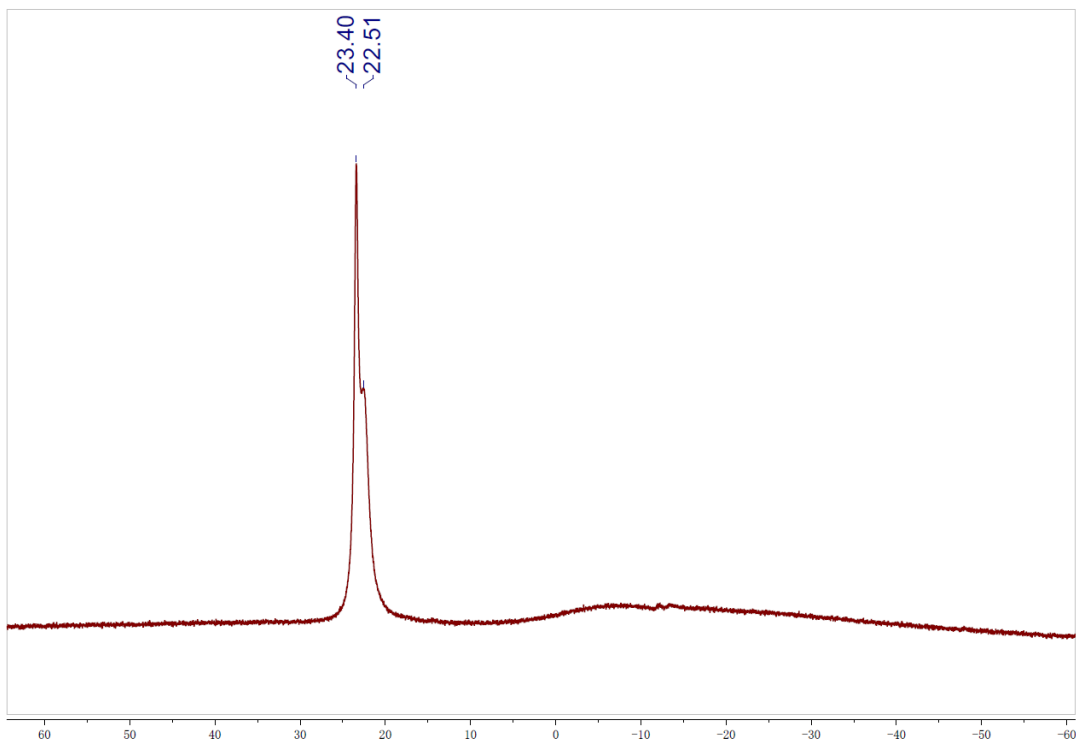


Fig S2 ^{11}B NMR spectrum of the clear solution after catalytic hydroboration of CO_2 with HBcat under complex **1**.

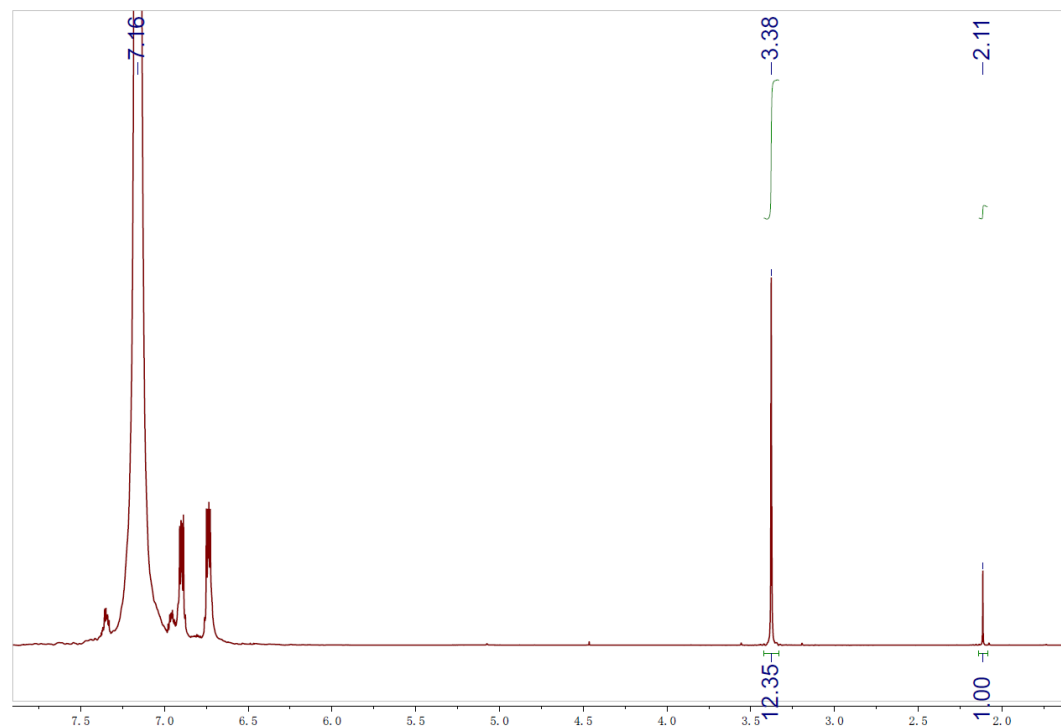


Fig S3 ^1H NMR spectrum of the clear solution after catalytic hydroboration of CO_2 with HBcat under complex **1**.

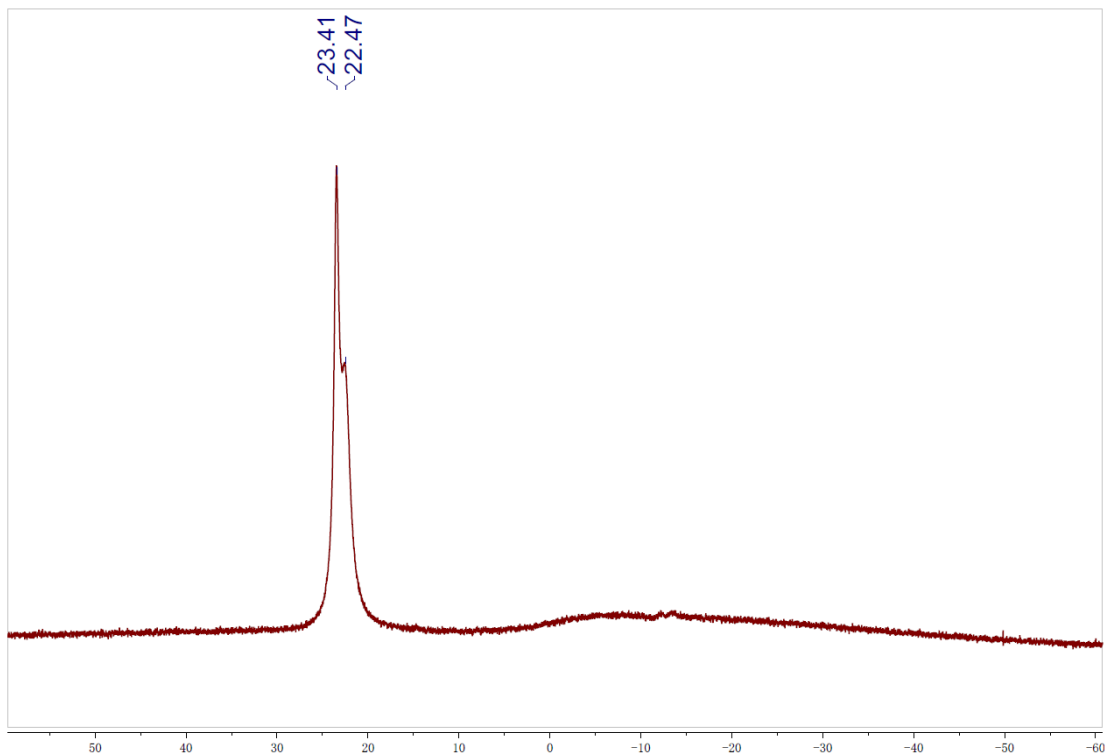


Fig S4 ^{11}B NMR spectrum of the clear solution after catalytic hydroboration of CO_2 with HBcat under complex **2**.

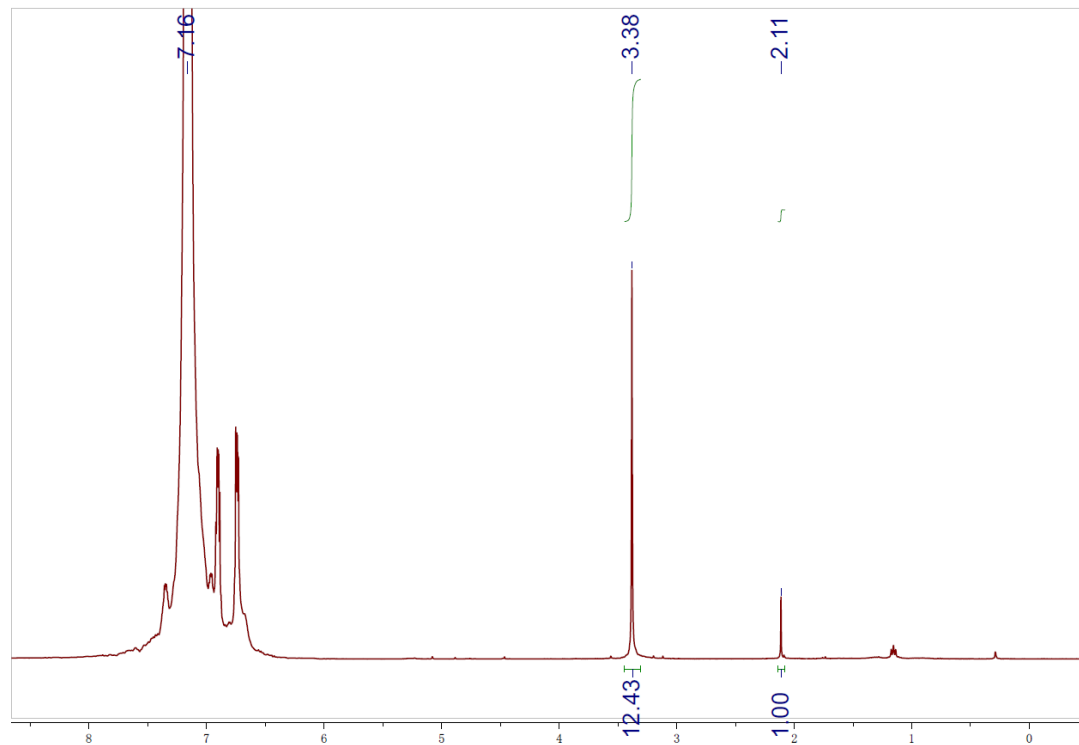


Fig S5 ^1H NMR spectrum of the clear solution after catalytic hydroboration of CO_2 with HBcat under complex **2**.

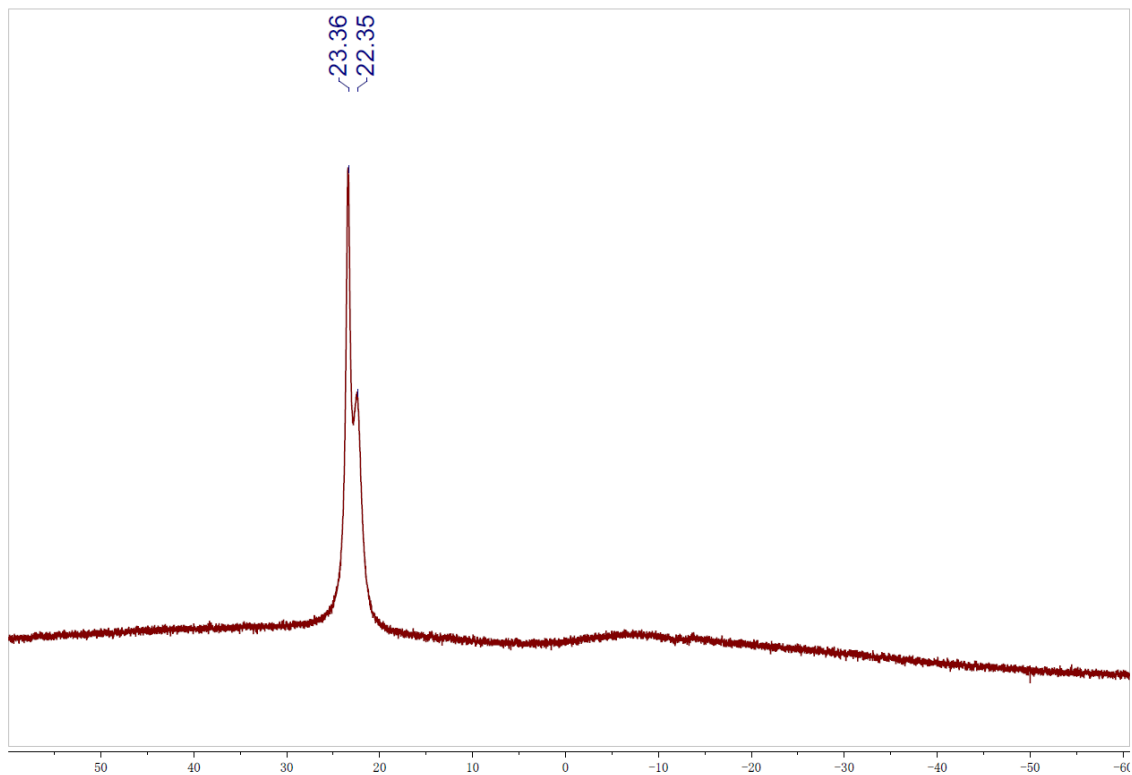


Fig S6 ^{11}B NMR spectrum of the clear solution after catalytic hydroboration of CO_2 with HBcat under complex **4**.

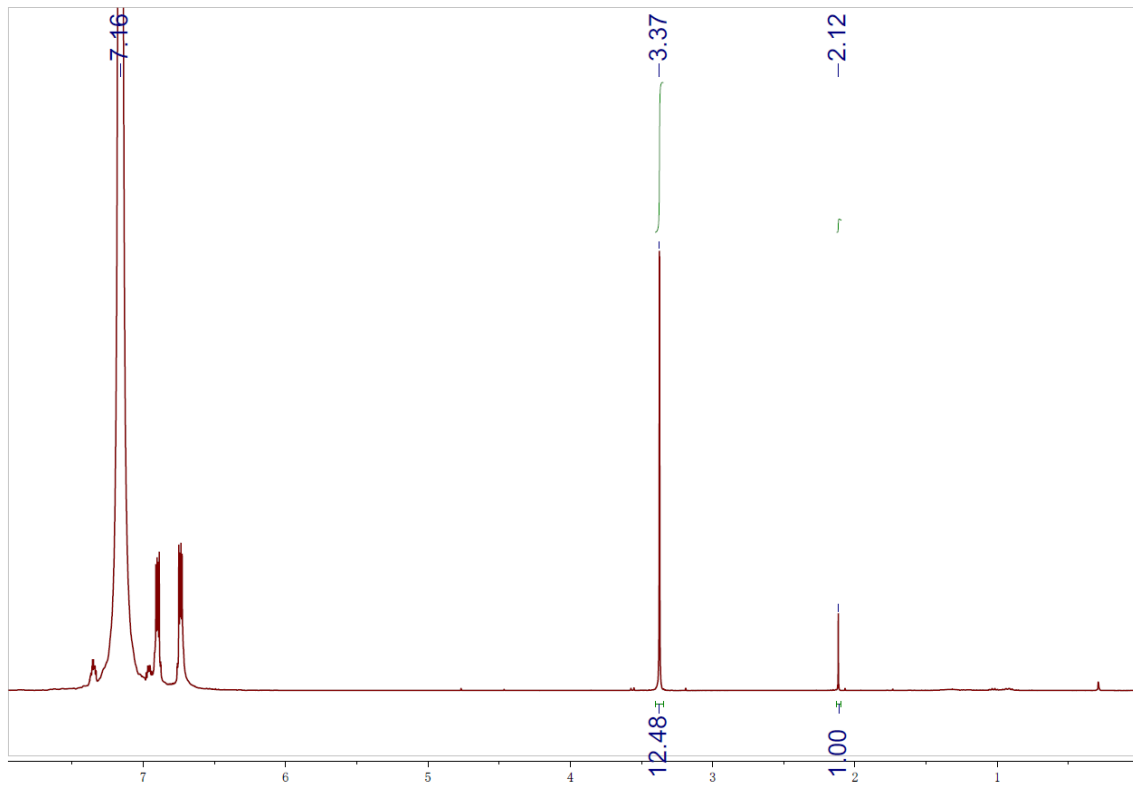


Fig S7 ^1H NMR spectrum of the clear solution after catalytic hydroboration of CO_2 with HBcat under complex **4**.

Reference:

1. A. V. Polukeev, S. A. Kuklin, P. V. Petrovskii, S. M. Peregudova, A. F. Smol'yakov, F. M. Dolgushin and A. A. Koridze, *Dalton Trans.*, 2011, **40**, 7201.
2. J.-F. Gong, Y.-H. Zhang, M.-P. Song and C. Xu, *Organometallics*, 2007, **26**, 6487.
3. A. Adhikary, J. R. Schwartz, L. M. Meadows, J. A. Krause and H. Guan, *Inorg. Chem. Front.* 2014, **1**, 71.